

1  
2  
3  
4  
5  
6  
7  
8  
9  
10  
11  
12  
13  
14  
15  
16  
17  
18  
19  
20  
21  
22  
23  
24  
25  
26  
27  
28  
29  
30  
31  
32  
33  
34

**A phylogenetic framework of the legume genus *Aeschynomene* for comparative genetic analysis of the Nod-dependent and Nod-independent symbioses**

**Laurent Brottier<sup>\*1</sup>, Clémence Chaintreuil<sup>\*1</sup>, Paul Simion<sup>2</sup>, Céline Scornavacca<sup>2</sup>, Ronan Rivallan<sup>3,4</sup>, Pierre Mournet<sup>3,4</sup>, Lionel Moulin<sup>5</sup>, Gwilym P. Lewis<sup>6</sup>, Joël Fardoux<sup>1</sup>, Spencer C. Brown<sup>7</sup>, Mario Gomez-Pacheco<sup>7</sup>, Mickaël Bourges<sup>7</sup>, Catherine Hervouet<sup>3,4</sup>, Mathieu Gueye<sup>8</sup>, Robin Duponnois<sup>1</sup>, Heriniaina Ramanankierana<sup>9</sup>, Herizo Randriambanona<sup>9</sup>, Hervé Vandrot<sup>10</sup>, Maria Zabaleta<sup>11</sup>, Maitrayee DasGupta<sup>12</sup>, Angélique D'Hont<sup>3,4</sup>, Eric Giraud<sup>1</sup> and Jean-François Arrighi<sup>\*\*1</sup>**

<sup>1</sup>IRD, Laboratoire des Symbioses Tropicales et Méditerranéennes, UMR LSTM, Campus International de Baillarguet, 34398 Montpellier, France, <sup>2</sup>Institut des Sciences de l'Evolution (ISE-M), Université de Montpellier, CNRS, IRD, EPHE, 34095 Montpellier Cedex 5, France, <sup>3</sup>CIRAD (Centre de Coopération Internationale en Recherche Agronomique pour le Développement), UMR AGAP, F-34398 Montpellier, France, <sup>4</sup>AGAP, Univ Montpellier, CIRAD, INRA, Montpellier SupAgro, 34060 Montpellier, France <sup>5</sup>IRD, Interactions Plantes Microorganismes Environnement, UMR IPME, 34394 Montpellier, France, <sup>6</sup>Comparative Plant and Fungal Biology Department, Royal Botanic Gardens, Kew, Richmond, Surrey, TW9 3AB, United Kingdom, <sup>7</sup>Institute of Integrative Biology of the Cell (I2BC), CEA, CNRS, Univ. Paris-Sud, Université Paris-Saclay, 91198, Gif-sur-Yvette, France, <sup>8</sup>Laboratoire de Botanique, Institut Fondamental d'Afrique Noire, Ch. A. Diop, BP 206 Dakar, Sénégal, <sup>9</sup>Laboratoire de Microbiologie de l'Environnement/Centre National de Recherche sur l'Environnement, Antananarivo 101, Madagascar, <sup>10</sup>IAC, Laboratoire de Botanique et d'Ecologie Végétale Appliquée, UMR AMAP, 98825 Pouembout, Nouvelle-Calédonie, <sup>11</sup>Department of Biochemistry and Microbial Genomics. IIBCE. Montevideo 11600. Uruguay, <sup>12</sup>Department of Biochemistry, University of Calcutta, Kolkata, 700019, India

\*: contributed equally to this work  
\*\*: Author for correspondence  
Jean-François Arrighi

35 Tel: +33 (0) 4 67 59 38 82

36 Fax: +33 (0) 4 67 59 38 02

37 E-mail: jean-francois.arrighi@ird.fr

38

39

40 Total word count: 6053

41 Introduction: 823

42 Materials and Methods: 1083

43 Results: 2601

44 Discussion: 1470

45 Acknowledgements: 76

46 Number of figures: 5 figures in color

47 Number of tables: 0

48 Supporting information: 12 figures and 4 tables

49

50

51

52

53

54

55

56

57

58

59

60

61

62

63

64

65

66

67

68

69 **SUMMARY**

70

71 • Some *Aeschynomene* legume species have the property of being nodulated by  
72 photosynthetic *Bradyrhizobium* lacking the *nodABC* genes. Knowledge of this unique Nod  
73 (factor)-independent symbiosis has been gained from the model *A. evenia* but our  
74 understanding remains limited due to the lack of comparative genetics with related taxa using  
75 a Nod-dependent process.

76 • To fill this gap, this study significantly broadened previous taxon sampling, including in  
77 allied genera, to construct a comprehensive phylogeny. This backbone tree was matched with  
78 data on chromosome number, genome size, low-copy nuclear genes and strengthened by  
79 nodulation tests and a comparison of the diploid species.

80 • The phylogeny delineated five main lineages that all contained diploid species while  
81 polyploid groups were clustered in a polytomy and were found to originate from a single  
82 paleo-allopolyploid event. In addition, new nodulation behaviours were revealed and Nod-  
83 dependent diploid species were shown to be tractable.

84 • The extended knowledge of the genetics and biology of the different lineages in the legume  
85 genus *Aeschynomene* provides a solid research framework. Notably, it enabled the  
86 identification of *A. americana* and *A. patula* as the most suitable species to undertake a  
87 comparative genetic study of the Nod-independent and Nod-dependent symbioses.

88

89

90

91

92

93

94

95

96

97

98

99 **Keywords**

100 *Aeschynomene*, genetics, legumes, nodulation, phylogenetics, polyploidy, symbiosis

101

102

103 **INTRODUCTION**

104

105 In the field of nitrogen-fixing symbiosis, scientists have a long-standing interest in the tropical  
106 papilionoid legume genus *Aeschynomene* since the discovery of the ability of the species *A.*  
107 *afraspera* to develop abundant nitrogen-fixing stem nodules (Hagerup, 1928). This nodulation  
108 behavior is uncommon in legumes, being shared by very few hydrophytic species of the  
109 genera *Discolobium*, *Neptunia* and *Sesbania*, but it is exceptionally widespread among the  
110 semi-aquatic *Aeschynomene* species (Alazard, 1985; Boivin *et al.*, 1997; Chaintreuil *et al.*,  
111 2013). These stem-nodulating *Aeschynomene* species are able to interact with *Bradyrhizobium*  
112 strains that display the unusual property of being photosynthetic (Giraud *et al.*, 2000; Miché  
113 *et al.*, 2010). Most outstanding is the evidence that some of these photosynthetic  
114 *Bradyrhizobium* strains lack both the *nodABC* genes required for the synthesis of the key  
115 “Nod factors” symbiotic signal molecules and a type III secretion system (T3SS) that is  
116 known in other rhizobia to activate or modulate nodulation (Giraud *et al.*, 2007; Okazaki *et*  
117 *al.*, 2013, 2015). These traits revealed the existence of an alternative symbiotic process  
118 between rhizobia and legumes that is independent of the Nod factors.

119 As in the legume genus *Arachis* (peanut), *Aeschynomene* uses an intercellular symbiotic  
120 infection process instead of infection thread formation that can be found in other legume  
121 groups (Sprent *et al.*, 2017). This led to the suggestion that the Nod-independent process  
122 might correspond to the ground state of the rhizobial symbiosis, although we cannot exclude  
123 that it represents an alternative symbiotic process compared to the one described in other  
124 legumes (Sprent & James, 2008; Madsen *et al.*, 2010, Okubo *et al.*, 2012). It is noteworthy  
125 that all the Nod-independent species form a monophyletic clade within the *Aeschynomene*  
126 phylogeny and jointly they also display striking differences in the bacteroid differentiation  
127 process compared to other *Aeschynomene* species (Chaintreuil *et al.*, 2013; Czernic *et al.*,  
128 2015). To decipher the molecular mechanisms of this distinct symbiosis, the Nod-independent  
129 *A. evenia* has been used as a new model legume, because its genetic and developmental  
130 characteristics (diploid with a reasonable genome size  $2n=20$ , 415 Mb/1C-, short perennial  
131 and autogamous, can be hybridized and transformed) make this species tractable for  
132 molecular genetics (Arrighi *et al.*, 2012, 2013, 2015). Functional analyses revealed that some  
133 symbiotic determinants identified in other legumes (*SYMRK*, *CCaMK*, *HK1* and *DNF1*) are  
134 recruited, but several key genes involved in bacterial recognition (e.g. *LYK3*), symbiotic  
135 infection (e.g. *EPR3* and *RPG*), and nodule functioning (e.g. *DNF2* and *FEN1*) were found  
136 not to be expressed in *A. evenia* roots and nodules, based on RNAseq data (Czernic *et al.*,

137 2015; Fabre *et al.*, 2015; Chaintreuil *et al.*, 2016a; Nouwen *et al.*, 2017). This suggested that  
138 the Nod-independent symbiosis is distinct from the Nod-dependent one.

139 Forward genetics are now expected to allow the identification of the specific molecular  
140 determinants of the Nod-independent process in *A. evenia* (Arrighi *et al.*, 2012; Chaintreuil *et*  
141 *al.*, 2016a). In addition, comparing *A. evenia* with closely related Nod-dependent  
142 *Aeschynomene* species will promote our understanding how symbiosis evolved in legumes.  
143 The genus *Aeschynomene* (restricted now to the section *Aeschynomene* as discussed in  
144 Chaintreuil *et al.* (2013)) is traditionally composed of three infrageneric taxa, subgenus  
145 *Aeschynomene* (which includes all the hydrophytic species) and subgenera *Bakerophyton* and  
146 *Rueppellia* (Rudd, 1955; Gillet *et al.*, 1971). The genus has also been shown to be  
147 paraphyletic, with a number of related genera being nested within it, but together they form a  
148 distinct clade in the tribe Dalbergieae (Chaintreuil *et al.*, 2013; Rudd, 1981; Lavin *et al.*,  
149 2001; Klitgaard *et al.*, 2005; LPWG, 2017). Within this broad clade, two groups of semi-  
150 aquatic *Aeschynomene* have been well-studied from a genetic and genomic standpoint: the *A.*  
151 *evenia* group, which contains all the Nod-independent species (most of them being 2x), and  
152 the *A. afraspera* group (all species being Nod-dependent) that appears to have a 4x origin  
153 (Arrighi *et al.*, 2014, Chaintreuil *et al.* 2016b, 2018). For comparative analyses, the use of  
154 Nod-dependent species with a diploid structure would be more appropriate, but such  
155 *Aeschynomene* species are poorly documented.

156 To overcome these limitations, our aim was to produce a species-comprehensive phylogenetic  
157 tree supplemented with genetic and nodulation data. For this, we made use of an extensive  
158 taxon sampling in both the genus *Aeschynomene* and in closely related genera to capture the  
159 full species diversity of the genus and to clarify phylogenetic relationships between taxa. For  
160 most species, we also documented chromosome number, genome size and molecular data for  
161 low-copy nuclear genes, thus allowing the identification of diploid species as well as  
162 untangling the genome structure of polyploid taxa. In addition, these species were  
163 characterized for their ability to nodulate with various *Bradyrhizobium* strains containing or  
164 lacking *nod* genes and, finally, the diploid species were submitted to a comparative analysis  
165 of their properties. In light of the data obtained in this study, we discuss the interest of two  
166 *Aeschynomene* species, *A. americana* and *A. patula*, to set up a comparative genetic system to  
167 complement the *A. evenia* model.

168

169

170 **MATERIALS & METHODS**

171

## 172 **Plant material**

173 All the accessions of *Aeschynomene* used in this study, including their geographic origin and  
174 collection data are listed in Tables S1 and S4. Seed germination and plant cultivation in the  
175 greenhouse were performed as indicated in Arrighi *et al.* (2012). Phenotypic traits such as the  
176 presence of adventitious root primordia and nodules on the stem were directly observed in the  
177 glasshouse.

178

## 179 **Nodulation tests**

180 Nodulation tests were carried out using *Bradyrhizobium* strains ORS278 (originally isolated  
181 from *A. sensitiva* nodules), ORS285 (originally isolated from *A. afraspera* nodules),  
182 ORS285 $\Delta$ *nod* and DOA9 (originally isolated from *A. americana* nodules) (Giraud *et al.*,  
183 2007; Teamtisong *et al.*, 2014; Bonaldi *et al.*, 2011). *Bradyrhizobium* strains were cultivated  
184 at 34°C for seven days in Yeast Mannitol (YM) liquid medium supplemented with an  
185 antibiotic when necessary (Howieson *et al.*, 2016). Plant *in vitro* culture was performed in  
186 tubes filled with buffered nodulation medium (BNM) as described in Arrighi *et al.* (2012).  
187 Five-day-old plants were inoculated with 1 mL of bacterial culture with an adjusted OD at  
188 600nm to 1. Twenty one days after inoculation, six plants were analysed for the presence of  
189 root nodules. Nitrogen-fixing activity was estimated on the entire plant by measurement of  
190 acetylene reducing activity (ARA) and microscopic observations were performed using a  
191 stereo-microscope (Nikon AZ100, Champigny-sur-Marne, France) as published in Bonaldi *et*  
192 *al.* (2011).

193

## 194 **Molecular methods**

195 Plant genomic DNA was isolated from fresh material using the classical CTAB (Cetyl  
196 Trimethyl Ammonium Bromide) extraction method. For herbarium material, the method was  
197 adapted by increasing the length of the incubation (90 min), centrifugation (20 min) and  
198 precipitation (15 min) steps. The nuclear ribosomal internal transcribed spacer region (ITS),  
199 the chloroplast *matK* gene and four low-copy nuclear genes (*CYP1*, *eiF1 $\alpha$* , *SuSy*, and *TIP1;1*)  
200 previously identified in the *A. evenia* and *A. afraspera* transcriptomes were used for  
201 phylogenetic analyses (Arrighi *et al.*, 2014; Chaintreuil *et al.*, 2016). The genes were PCR-  
202 amplified, cloned and sequenced as described in Arrighi *et al.* (2014) (Table S2). For genomic  
203 DNA extracted from herbarium specimens, a battery of primers was developed to amplify the

204 different genes in overlapping fragments as short as 250 bp (Table S2). The DNA sequences  
205 generated in this study were deposited in GenBank (Table S3).

206

### 207 **Phylogenetic analyses and traits mapping**

208 Sequences were aligned using MAFFT (*--localpair --maxiterate 1000*; Katoh & Standley,  
209 2013). Phylogenetic reconstructions were performed for each gene as well as for concatenated  
210 datasets under a Bayesian approach using Phylobayes 4.1b (Lartillot & Philippe, 2004) and  
211 the site-heterogeneous CAT+F81+F4 evolution model. For each analysis, two independent  
212 chains were run for 10,000 Phylobayes cycles with a 50% burn-in. Ancestral states  
213 reconstruction was done through stochastic character mapping using the Phytools R package  
214 (Revell, 2012) running 10 simulations for each character.

215

### 216 **Species networks and hybridizations**

217 To test if the phylogeny obtained by concatenating the four low-copy nuclear genes (*CYP1*,  
218 *eiFla*, *SuSy*, and *TIP1;1*) was most likely obtained by gene duplications followed by  
219 differential losses or by a combination of duplications, losses coupled with one or several  
220 allopolyploidy events involving *A. patula* and *Soemmeringia semperflorens*, the method  
221 presented in To & Scornavacca (2015) was used. In short, this method computes a  
222 reconciliation score by comparing a phylogenetic network and one or several gene trees. The  
223 method allows allopolyploidy events at hybridization nodes while all other nodes of the  
224 network are associated to speciation events; meanwhile, duplication and loss events are  
225 allowed at a cost (here, arbitrarily fixed to 1) on all nodes of the gene tree.

226 Thus, the set of 4 nuclear gene trees was used to score different phylogenetic networks  
227 corresponding to four different potential evolutionary histories. Two alternative networks with  
228 no reticulation corresponding to the two topologies obtained either with the group A (T1) or  
229 group B (T2) served to evaluate a no-allopolyploidisation hypothesis. The topology yielding  
230 the best score (T2) served to generate and compare all phylogenetic networks with one or two  
231 hybridization nodes, involving *A. patula* and/or *S. semperflorens*, to test successively a one-  
232 allopolyploidisation scenario (N1-best) and a two-allopolyploidisation evolutionary scenario  
233 (N2-best).

234

### 235 **GBS analysis**

236 A GBS library was constructed based on a described protocol (Oueslati *et al.*, 2017). For each  
237 sample, a total of 150 ng of genomic DNA was digested using the two-enzyme system, PstI

238 (rare cutter) and Mse (common cutter) (New England Biolabs, Hitchin, UK), by incubating at  
239 37°C for 2 h. The ligation reaction was performed using the T4 DNA ligase enzyme (New  
240 England Biolabs, Hitchin, UK) at 22°C for 30 min and the ligase was inactivated at 65°C for  
241 30 min. Ligated samples were pooled and PCR-amplified using the Illumina Primer 1  
242 (barcoded adapter with PstI overhang) and Illumina Primer 2 (common Y-adapter). The  
243 library was sequenced on an Illumina HiSeq 3000 (1x 150 pb) (at the Get-PlaGe platform in  
244 Toulouse, France).

245 The raw sequence data were processed in the same way as in the study described in Garsmeur  
246 *et al.* (2018). SNP calling from the raw Illumina reads was performed using the custom  
247 python pipeline VcfHunter (available at <https://github.com/SouthGreenPlatform/VcfHunter/>)  
248 (Guillaume Martin, CIRAD, France). For all samples, these sequence tags were aligned to the  
249 *A. evenia* 1.0 reference genome (JF Arrighi, unpublished data). The SNP results from all the  
250 samples were converted into one large file in VCF format and the polymorphism data were  
251 subsequently analysed using the web-based application SNIPlay3 (Dereeper *et al.*, 2015).  
252 First, the SNP data were treated separately for each species and filtered out to remove SNP  
253 with more than 10% missing data as well as those with a minor allele frequency (MAF) of  
254 0.01 using integrated VCFtools. Second, an overall representation of the species diversity  
255 structures was obtained by making use of the PLINK software as implemented in SNIPlay3.  
256 This software is based on the multidimensional-scaling (MSD) method to produce two-  
257 dimensional plots. The Illumina HiSeq 3000 sequencing raw data are available in the NCBI  
258 SRA (Sequence Read Archive) under the study accession number: SRP149516.

259

### 260 **Genome size estimation and chromosome counting**

261 Genome sizes were measured by flow cytometry using leaf material as described in Arrighi *et*  
262 *al.* (2012). Genome size estimations resulted from measurements of three plants per accession  
263 and *Lycopersicon esculentum* (Solanaceae) cv “Roma” (2C = 1.99 pg) was used as the  
264 internal standard. The 1C value was calculated and the conversion factor 1 pg DNA = 978 Mb  
265 was used to express it in Mb/1C. To count chromosome number, metaphasic chromosomes  
266 were prepared from root-tips, spread on slides, stained with 4',6-diamidino-2-phenylindole  
267 (DAPI) and their image captured with a fluorescent microscope as detailed in Arrighi *et al.*  
268 (2012) .

269

270

## 271 **RESULTS**



272

273 **A comprehensive phylogeny of the genus *Aeschynomene* and allied genera**

274 To obtain an in-depth view of the phylogenetic relationships within the genus *Aeschynomene*  
275 subgenus *Aeschynomene*, which contains the hydrophytic species, we significantly increased  
276 previous sampling levels by the addition of new germplasm accessions and, if these were not  
277 available, we used herbarium specimens. DNA was isolated for 40 out of the 41 species  
278 (compared to the 27 species used in Chaintreuil *et al.* (2013)) included in this group in  
279 taxonomic and genetic studies (Table S1) (Arrighi *et al.*, 2014; Chaintreuil *et al.*, 2012,  
280 2016b, 2018; Rudd, 1955). In addition, to determine the phylogenetic relationship of this  
281 subgenus with respect to *Aeschynomene* subgenera *Bakerophyton* and *Rueppellia*, unclassified  
282 *Aeschynomene* species, as well as with the allied genera *Bryaspis*, *Cyclocarpa*, *Geissaspis*,  
283 *Humularia*, *Kotschya*, *Smithia* and *Soemmeringia*, representatives of these 10 taxa were also  
284 sampled (compared to the 5 taxa present in Chaintreuil *et al.* (2013)) (Rudd, 1981; Lewis,  
285 2005). This added 21 species to our total samples (Table S1). The dalbergioid species *Pictetia*  
286 *angustifolia* was used as outgroup (Chaintreuil *et al.* 2013; LPWG, 2017).

287 Phylogenetic reconstruction of all the taxa sampled was undertaken using Bayesian analysis  
288 of the chloroplast *matK* gene and the nuclear ribosomal *ITS* region (Table S2 and S3). The  
289 *matK* and *ITS* gene trees distinguished almost all the different *Aeschynomene* groups and  
290 related genera (Fig. S1 and S2). The two phylogenetic trees have a very similar topology  
291 although some branches of both trees can be lowly supported. Incongruences were also  
292 observed for *A. deamii* and the genus *Bryaspis*, but the conflicting placements are poorly  
293 supported and were thus interpreted as a lack of resolution typical of single-marker trees,  
294 rather than strong incongruence. To improve the phylogenetic resolution among the major  
295 lineages, the *matK* gene and the *ITS* sequence datasets were combined into a single  
296 phylogenetic analysis where only well-supported nodes were considered (posterior probability  
297 (PP)  $\geq 0.5$ ) (Fig. 1). Our analysis recovered a grade of five main lineages with a branching  
298 order that received robust support (PP  $\geq 0.92$ ): (1) a basally branching lineage represented by  
299 *A. americana*, (2) an *A. montevidensis* lineage, (3) an *A. evenia* lineage corresponding to the  
300 Nod-independent clade (Arrighi *et al.*, 2012, 2014), (4) a newly-identified lineage containing  
301 *A. patula* and (5) a lineage represented by an unresolved polytomy clustering the *A. afraspera*  
302 clade (Chaintreuil *et al.*, 2016b) with all the remaining taxa.

303 In large part, our work also provided good species-level resolution and demonstrated that  
304 *Aeschynomene* subgenus *Aeschynomene* (as currently circumscribed) is interspersed on the  
305 phylogenetic tree with the lineage containing *A. patula*, the two other subgenera of

306 *Aeschynomene* and a number of other genera related to *Aeschynomene* (Fig. 1) (Chaintreuil *et*  
307 *al.*, 2013; Lavin *et al.*, 2001; LPWG, 2017; Du Puy *et al.*, 2002). The combined analysis also  
308 grouped the genus *Bryaspis* with the species related to *A. afraspera* in a highly supported  
309 clade but its exact position with respect to other taxa remained inconclusive, as previously  
310 observed (Fig. 1) (Chaintreuil *et al.*, 2013). Most noticeably, several intergeneric relationships  
311 are consistently recovered, notably sister-clade relationships between *Cyclocarpa* and *Smithia*  
312 as well as between *Aeschynomene* subgenera *Bakerophyton* and *Rueppellia* together with the  
313 genus *Humularia* (referred to as the BRH clade herein after) (Fig. 1). This clade supports  
314 previous observations of a morphological continuum between *Aeschynomene* subgenus  
315 *Rueppellia* and the genus *Humularia* and brings into question their taxonomic separation  
316 (Gillett *et al.*, 1971).

317

### 318 **Ploidy level of the species and genomic structure of the different lineages**

319 The revised *Aeschynomene* phylogeny was used as a backbone tree to investigate the  
320 evolution of ploidy levels. Previous studies had demonstrated that the *A. evenia* clade is  
321 mostly diploid ( $2n=2x=20$ ) even if some species such as *A. indica* ( $2n=4x=40$ ,  $2n=6x=60$ )  
322 appear to be of recent allopolyploid origin (Arrighi *et al.*, 2014; Chaintreuil *et al.*, 2018).  
323 Conversely, all the species of the *A. afraspera* group were found to be polyploid  
324 ( $2n=4x=28,38,40$ ,  $2n=8x=56,76$ ) and to have a common AB genome structure but the origin  
325 of the polyploidy event remained undetermined (Chaintreuil *et al.*, 2016b). To assess the  
326 ploidy levels in *Aeschynomene* species and related genera, chromosome numbers and nuclear  
327 DNA content were determined (appended to labels in Fig. 2a, Table S1, Fig. S3 and S4). We  
328 provide evidence that the lineages containing *A. americana*, *A. montevidensis*, *A. evenia* and  
329 *A. patula*, as well as *Soemmeringia semperflorens*, are diploid with  $2n=20$ , with the smallest  
330  $2x$  genome found in *A. patula* (0.58 pg/2C) and the largest  $2x$  genome in *A. deamii* (1.93  
331 pg/2C). With the exception of *S. semperflorens*, all the groups that are part of the polytomy  
332 were characterized by higher chromosome numbers  $2n=28,36,38,40$  (up to 76). These  
333 chromosome numbers equate to approximately twice that of the diploid species (except for  
334  $2n=28$ ), suggesting that the corresponding groups are most probably polyploid. Species with  
335 chromosome numbers departing from  $2n=40$  are likely to be of dispolyploid origin as already  
336 described in the *A. afraspera* clade (Chaintreuil *et al.*, 2016b). Here again, important genome  
337 size variations ranging from 0.71 pg/2C for the *Geissaspis* species to 4.82 pg/2C for the  $4x$  *A.*  
338 *schimperii* highlight the genomic differentiation of the various taxa (Fig. 2a, Table S1).

339 To firmly link chromosome numbers to ploidy levels and to clarify genetic relationships  
340 between the different lineages, we cloned and sequenced four nuclear-encoded low-copy  
341 genes in selected species: *CYPI* (Cyclophilin 1), *eiFl $\alpha$*  (eukaryotic translation initiation factor  
342  $\alpha$ ), *SuSy* (Sucrose Synthase) and *TIP1;1* (tonoplast intrinsic protein 1;1) (Table S2). For all  
343 diploid species, only one gene sequence was obtained, while for all the polyploid species, in  
344 almost all cases, a pair of putative homeologues was isolated, thus confirming their genetic  
345 status inferred from the karyotypic data (Table S3). In general, the duplicated copies were  
346 highly divergent and nested in two different major clades in the resulting Bayesian phylogenic  
347 trees generated for each gene (Fig. S5). One clade contained all the A copies (except for one  
348 anomalous sequence for *Bryaspis lupulina* in the *eiFl $\alpha$*  tree) and the other clade gathered all  
349 the B copies previously identified in *A. afraspera* (Chaintreuil *et al.*, 2016b). These two  
350 clades A and B did not always receive high support, however it is notable that the A copies  
351 formed a monophyletic group with, or sister to, the *A. patula* sequence and similarly the B  
352 copies with, or sister to, the *Soemmerignia semperflorens* sequence, in all gene trees (Fig. S5).  
353 In an attempt to improve phylogenetic resolution, the four gene data sets were concatenated.  
354 This combination resulted in a highly supported Bayesian tree that places the A copy clade as  
355 the sister to the diploid *A. patula* (PP =1), and the B copy clade as sister to the diploid *S.*  
356 *semperflorens* (PP =1) (Fig. 2b). As a result, these phylogenetic analyses combined to  
357 karyotypic data show that all the five main lineages contain diploid species. They also reveal  
358 that all the polyploid groups share the same AB genome structure, with the diploid *A. patula*  
359 and *S. semperflorens* species being the closest modern representatives of the ancestral donors  
360 of the A and B genomes.

361 In addition, an ancestral state reconstruction analysis performed on the *ITS+matK* phylogeny  
362 indicates that diploidy is the ancestral condition in the whole revised group and that  
363 tetraploidy most likely evolved once in the polytomy (Fig. S6). To provide support on a  
364 probable single origin of the allopolyploidy event, separate and concatenated nuclear gene  
365 trees were further used for a phylogenetic network analysis. In this analysis, the two non-  
366 allopolyploidisation hypotheses (T1 and T2) were found to be more costly (scores of 207 and  
367 196) than the two hypotheses allowing for hybridization (N1-best and N2-best with scores of  
368 172 and 169, respectively) (Fig. S7a-d). The one-allopolyploidisation hypothesis (N1-best)  
369 strongly indicates that a hybridization involving the lineages that contain *A. patula* and *S.*  
370 *semperflorens* gave rise to all the polyploid groups (Fig. S7c). Although the two-  
371 allopolyploidisation hypothesis (N2-best) yielded the absolute best score, the score  
372 improvement was very low (169 vs 172) and the resulting network included the hybridization

373 inferred with the one-allopolyploidisation hypothesis making this latter hypothesis most  
374 probably the correct one (Fig. S7d).

375

### 376 **Nodulation properties of the different *Aeschynomene* lineages**

377 Species of *Aeschynomene* subgenus *Aeschynomene* are known to be predominantly  
378 amphibious and more than 15 of these hydrophytic species (found in the *A. evenia* and *A.*  
379 *afraspera* clades, as well as *A. fluminensis*) have been described as having the ability to  
380 develop stem nodules (Boivin *et al.*, 1997; Chaintreuil *et al.*, 2016b; Lock, 1989; Rudd,  
381 1955). In *A. fluminensis*, these nodules are observed only on submerged stems (as also seen in  
382 the legume *Discolobium pulchellum*), while they occur on aerial stems within the *A. evenia*  
383 and *A. afraspera* clades (Fig. 3a) (Alazard & Duhoux, 1987; Chaintreuil *et al.*, 2013; Loureiro  
384 *et al.*, 1994, 1995). Phenotypic analysis of representatives of the different lineages under  
385 study revealed that they all display adventitious root primordia along the stem (Fig. 3a,b).  
386 Adventitious roots are considered to be an adaptation to temporary flooding and they also  
387 correspond to nodulation sites in stem-nodulating *Aeschynomene* species (Fig. 3b) (Alazard &  
388 Duhoux, 1987). Given that the *A. evenia* and *A. afraspera* clades are now demonstrated not to  
389 share the same genomic components provides a genetic argument for independent  
390 developments of stem nodulation by photosynthetic bradyrhizobia. Reconstruction of  
391 ancestral characters based on the *ITS+matK* phylogeny confirmed that the whole group was  
392 ancestrally a wet ecology taxon endowed with adventitious root primordia but that the stem  
393 nodulation ability evolved several times, as previously inferred (Fig. S8, S9; and S10)  
394 Chaintreuil *et al.*, 2013, 2016b).

395 To investigate whether the newly studied species could be nodulated by photosynthetic  
396 bradyrhizobia, we extended the results obtained by Chaintreuil *et al.* (2013) by testing the  
397 nodulation abilities of 22 species available (listed in Fig. 4a) for which adequate seed supply  
398 was available. Three different strains of *Bradyrhizobium* equating to the three cross-  
399 inoculation (CI) groups defined by Alazard (1985) were used: DOA9 (non-photosynthetic  
400 *Bradyrhizobium* of CI-group I), ORS285 (photosynthetic *Bradyrhizobium* with *nod* genes of  
401 CI-group II) and ORS278 (photosynthetic *Bradyrhizobium* lacking *nod* genes of CI-group  
402 III). These strains were used to inoculate the 22 species and their ability to nodulate them was  
403 analysed at 21 dpi. For this, we recorded nodule formation and compared nitrogen fixation  
404 efficiency by an acetylene reduction assay (ARA) and observation of plant vigor. Nodulation  
405 was observed on all species tested except for *Smithia sensitiva* that had a problem with root

406 development, *A. montevidensis* and *S. semperflorens*. For these three species, either the  
407 culture conditions or the *Bradyrhizobium* strains used were not appropriate (Fig. 4a).  
408 The non-photosynthetic strain DOA9 displayed a wide host spectrum but was unable to  
409 nodulate the Nod-independent species, *A. deamii*, *A. evenia* and *A. tambacoundensis*. The  
410 photosynthetic strain ORS285 efficiently nodulated *A. afraspera* and the Nod-independent  
411 *Aeschynomene* species (Fig 4a), as previously reported (Chaintreuil *et al.*, 2013).  
412 Interestingly, the ORS285 strain was also able to induce nitrogen-fixing nodules in *A. patula*  
413 and ineffective nodules were observed on *A. fluminensis* and the genera *Bryaspis*, *Cyclocarpa*  
414 and *Smithia* (Fig. 4a). To examine if in these species the nodulation process relies on a Nod-  
415 dependent or Nod-independent symbiotic process, we took advantage of the availability of a  
416  $\Delta nod$  mutant of the strain ORS285. None of them were found to be nodulated by  
417 ORS285 $\Delta nod$ , suggesting that the nodule formation depended on a Nod signaling in these  
418 species (Fig. 4a). In fact, the ORS285 $\Delta nod$  mutated strain was able to nodulate only species  
419 of the *A. evenia* clade, similarly as to the photosynthetic strain ORS278 naturally lacking *nod*-  
420 genes (Fig. 4a). Analysis of the evolution of these nodulation abilities by performing an  
421 ancestral state reconstruction on the revisited phylogeny indicated several emergences of the  
422 ability to interact with photosynthetic bradyrhizobia and a unique emergence of the ability to  
423 be nodulated by the *nod* gene-lacking strain as observed earlier (Fig. S11 and Fig. S12)  
424 (Chaintreuil *et al.*, 2013). From these nodulation tests, different nodulation patterns emerged  
425 for the diploid *Aeschynomene* species (as detailed in Fig. 4b-d) with the DOA9 and ORS278  
426 strains being specific to the Nod-dependent and Nod-independent groups respectively and  
427 ORS285 showing a gradation of compatibility between both.

428

#### 429 **Diversity of the diploid species outside the Nod-independent clade**

430 To further characterize the diploid species that fall outside of the Nod-independent clade, in  
431 which *A. evenia* lies, they were analysed for their developmental properties and genetic  
432 diversity (Fig. 5a). All species are described as annuals or short-lived perennials (Du Puy *et*  
433 *al.*, 2002; Lewis, 2005; Rudd, 1955). As for *A. evenia*, *A. americana*, *A. villosa*, *A.*  
434 *fluminensis*, *A. parviflora* and *A. montevidensis* are robust and erect, reaching up to 2 m high  
435 when mature, whilst *A. patula* and *S. semperflorens* are creeping or decumbent herbs. These  
436 differences in plant habit are reflected by the important variation in seed size between these  
437 two groups (Fig. 5a). This has an impact on plant manipulation, because for *A. patula* and *S.*  
438 *semperflorens* seed scarification needs to be adapted (25 min with concentrated sulfuric acid  
439 instead of 40 min for the other species) and *in vitro* plant growth takes slightly more time to

440 get a root system sufficiently developed for inoculation with *Bradyrhizobium* strains (10 days-  
441 post-germination instead of the 5-7 dpi for other species) (Arrighi *et al.*, 2012). Consistent  
442 flowering and seed production was observed for *A. americana*, *A. villosa*, *A. patula* and *S.*  
443 *semperflorens* when grown under full ambient light in the tropical greenhouse in short days  
444 conditions as previously described for *A. evenia*, making it possible to develop inbred lines by  
445 successive selfing (Fig. 5a) (Arrighi *et al.*, 2012). For *A. fluminensis*, *A. parviflora* and *A.*  
446 *montevidensis*, flowering was sparse or not observed, indicating that favorable conditions for  
447 controlled seed set were not met (Fig. 5a).

448 Five species (*A. villosa*, *A. fluminensis*, *A. parviflora*, *A. montevidensis* and *S. semperflorens*)  
449 are strictly American while *A. americana* is a pantropical species and *A. patula* is endemic to  
450 Madagascar (Du Puy *et al.*, 2002; Lock, 1989; Rudd, 1955). Several species have a narrow  
451 geographic distribution or seem to be infrequent, explaining the very limited accession  
452 availability in seedbanks (Fig. 5a). This is in sharp contrast with both *A. americana* and *A.*  
453 *villosa* that are well-collected, being widely found as weedy plants and sometimes used as  
454 component of pasture for cattle (Fig. 5a) (Cook *et al.*, 2005). To assess the genetic diversity of  
455 these two species, a germplasm collection containing 79 accessions for *A. americana* and 16  
456 accessions for *A. villosa*, and spanning their known distribution was used (Table S4). A  
457 Genotyping-By-Sequencing (GBS) approach resulted in 6370 and 1488 high quality  
458 polymorphic SNP markers for *A. americana* and *A. villosa* accessions, respectively. These  
459 two SNP datasets subsequently served for a clustering analysis based on the  
460 multidimensional-scaling (MSD) method. The MSD analysis distinguished three major  
461 groups of accessions for both *A. americana* and *A. villosa* along coordinate axes 1 and 2 (Fig.  
462 5b). When mapping the accessions globally, the three groups identified for *A. villosa* were  
463 observed together in Mexico and only group (3) extended to the northern part of South  
464 America (Fig. 5c, Table S4). Conversely, a clear geographical division was observed for *A.*  
465 *americana* with group (1) occupying the central part of South America, group (2) being found  
466 in the Caribbean area while group (3) was present in distinct regions from Mexico to Brazil  
467 and in across the Palaeotropics (Fig. 5c, Table S4). *A. americana* is hypothesized to be native  
468 in America and naturalized elsewhere (Cook *et al.*, 2005). The observed distributions in  
469 combination with the MSD analysis, accessions being tightly clustered in group (3) compared  
470 to groups (1) and (2), support this idea and indicate that group (3) recently spread worldwide.

471

472

473 **DISCUSSION**



474

475 **A well-documented phylogenetic framework for the legume genus *Aeschynomene***

476 We produced a new and comprehensive phylogeny of the genus *Aeschynomene* and its closely  
477 related genera complemented by gene data sets, genome sizes, karyotypes and nodulation  
478 assays. For plant genera, there are few for which documentation of taxonomic diversity is so  
479 extensive and supported by a well-resolved, robustly supported phylogeny which reveals the  
480 evolutionary history of the group (Govindarajulu *et al.*, 2011). Here, the whole group, which  
481 includes the genus *Aeschynomene* with its 3 subgenera and its 7 allied genera, is shown to  
482 have experienced cladogenesis leading to five main lineages, including the Nod-independent  
483 clade, with diploid species found in all these lineages. The multigene data analysis provided  
484 robust evidence that two of them, represented by the two diploid species *A. patula* and *S.*  
485 *semperflorens*, are involved in an ancient allotetraploidization process that gave rise to the  
486 different polyploid lineages clustering in a polytomy. Separate allopolyploidization events  
487 from the same diploid parents or a single allopolyploid origin are plausible explanations for  
488 the formation of these lineages. However, the consistent resolution of the phylogenetic tree  
489 obtained with the combined gene data, where *A. patula* and *S. semperflorens* are sisters to the  
490 A and B subgenomic sequences, favours the hypothesis of a single allopolyploid origin, as  
491 also argued for other ancient plant allopolyploid events in *Asimitellaria* (Saxifragaceae) and  
492 *Leucaena* (Leguminosae) (Govindarajulu *et al.*, 2011; Okuyama *et al.*, 2012). The  
493 phylogenetic network analysis also supports the one-allopolyploidisation hypothesis.  
494 However, additional nuclear genes will be needed to conclusively confirm that no additional  
495 hybridization event occurred. Although not the focus of the present study, it is worth noting  
496 that most diploid species are found in the Neotropics, the two modern representatives of the A  
497 and B genome donors that gave rise to the 4x lineages are located on different continents (*S.*  
498 *semperflorens* in South America and *A. patula* in Madagascar) and that all the 4x lineages are  
499 located in the Palaeotropics (Lewis *et al.*, 2005). This raises questions about the evolution of  
500 the whole group and the origin of the 4x lineages. In addition, the presence of a polytomy  
501 suggests that this allopolyploid event preceded a rapid and major diversification of 4x groups  
502 that have been ascribed to different *Aeschynomene* subgenera or totally distinct genera that  
503 altogether represent more than 80% of the total species of the whole group (LPWG, 2017;  
504 Whitefiel & Lockhart, 2007). Diversification by allopolyploidy occurred repeatedly in the  
505 genus *Aeschynomene* since several neopolyploid species are found in both the *A. evenia* clade  
506 and the *A. afraspera* clade as exemplified by *A. indica* (4x, 6x) and *A. afraspera* (8x) (Arrighi  
507 *et al.*, 2014; Chaintreuil *et al.*, 2016b). Dense sampling for several *Aeschynomene* taxa or

508 clades also a more precise delimitation of species boundaries (for morphologically similar  
509 taxa but which are genetically differentiated or correspond to different cytotypes) and  
510 revealed intraspecific genetic diversity that is often geographically-based as showed for the  
511 pantropical species *A. americana* (this study), *A. evenia*, *A. indica* and *A. sensitiva*  
512 (Chaintreuil *et al.*, 2018). All these *Aeschynomene* species share the presence of adventitious  
513 root primordia on the stem that correspond to the infection sites for nodulation. The consistent  
514 presence of adventitious root primordia in all taxa of the whole group, together with an  
515 ancestral state reconstruction, substantiates the two-step model proposed earlier for the  
516 evolution of stem nodulation in *Aeschynomene*, with a common genetic predisposition at the  
517 base of the whole group to produce adventitious root primordia on the stem, as an adaptation  
518 to flooding, and subsequent mutations occurring independently in various clades to enable  
519 stem nodulation (Chaintreuil *et al.*, 2013). The ability to interact with photosynthetic  
520 bradyrhizobia that are present in aquatic environments also appears to have evolved several  
521 times. This photosynthetic activity is important for the bacterial symbiotic lifestyle as it  
522 provides energy usable for infection and subsequently for nitrogenase activity inside the stem  
523 nodules (Giraud *et al.*, 2000). To date, natural occurrence of nodulation by photosynthetic  
524 bradyrhizobia has been reported only for the *A. evenia* and *A. afraspera* clades, and for *A.*  
525 *fluminensis* (Loureiro *et al.*, 1995; Miché *et al.*, 2010; Molouba *et al.*, 1997). Nevertheless, we  
526 could not test the photosynthetic strains isolated from *A. fluminensis* nodules and the nature of  
527 the strains present in those of the newly studied species *A. patula* has not been investigated  
528 yet. They would allow the comparison of their nodulation efficiency with the reference  
529 photosynthetic *Bradyrhizobium* ORS278 and ORS285 strains. In addition, we can ask if the  
530 semi-aquatic lifestyle and/or nodulation with photosynthetic bradyrhizobia may have  
531 facilitated the emergence of the Nod-independent symbiosis in the *A. evenia* clade.

532

### 533 ***Aeschynomene* species for a comparative analysis of nodulation with *A. evenia***

534 To uncover whether the absence of detection for several key symbiotic genes in the root and  
535 nodule transcriptomic data of *A. evenia* are due to gene loss or extinction, and to identify the  
536 specific symbiotic determinants of the Nod-independent symbiosis, a genome sequencing  
537 combined with a mutagenesis approach is presently being undertaken for *A. evenia* in our  
538 laboratory. A comparative analysis with Nod-dependent *Aeschynomene* species is expected to  
539 consolidate this genomic and genetic analysis performed in *A. evenia* by contributing to  
540 elucidate the genetic changes that enabled the emergence of the Nod-independent process.  
541 Phylogenomics and comparative transcriptomics, coupled with functional analysis, are



542 undergoing increased development in the study of symbiosis. They enabled unravelling gene  
543 loss linked to the lack of developing a symbiosis in certain plant lineages but also to identify  
544 new symbiosis genes (for arbuscular mycorrhizal symbiosis (Delaux *et al.*, 2014; Bravo *et al.*,  
545 2016); for the nodulating symbiosis (Delaux *et al.*, 2015; Griesmann *et al.*, 2018).  
546 Comparative work on symbiotic plants is often hindered, however, either by the absence of  
547 closely related species which display gain or loss of symbiotic function or, when these are  
548 present, by the lack of a well-understood genetic framework, as outlined in Behm *et al.*  
549 (2014), Delaux *et al.* (2015), Geurts *et al.* (2016), Sprent (2017). Nevertheless, in the case of  
550 the nodulating *Parasponia*/non-nodulating *Trema* system, a fine comparative analysis was  
551 very powerful to demonstrate a parallel loss of the key symbiotic genes *NFR5*, *NIN* and *RGP*,  
552 in the non-nodulating species, challenging the long-standing assumption that *Parasponia*  
553 specifically acquired the potential to nodulate (Behm *et al.*, 2014; Geurts *et al.*, 2016; van  
554 Velzen *et al.*, 2018). In this respect, the uncovering of the genetic evolution of the genus  
555 *Aeschynomene* and related genera along with the identification of diploid species outside of  
556 the Nod-independent clade, provided a robust phylogenetic framework that can now be  
557 exploited to guide the choice of Nod-dependent diploid species for comparative genetic  
558 research. Among these, some species are discarded because of the lack of nodulation with  
559 reference *Bradyrhizobium* strains or the inability to produce seeds under greenhouse  
560 conditions. Based on efficient nodulation, short flowering time and ease of seed production,  
561 *A. americana* (2n=20, 600 Mb) and *A. patula* (2n=20, 270 Mb) appear to be the most  
562 promising Nod-dependent diploid species to develop a comparative genetic system with *A.*  
563 *evenia* (2n=20, 400 Mb). In contrast to *A. evenia*, *A. americana* is nodulated only by non-  
564 photosynthetic bradyrhizobia, and in this respect, it behaves in a similar way to other legumes.  
565 This species is widespread in the tropics, so that adequate quantities of germplasm are  
566 available, and it has already been subject to detailed studies, notably to isolate its nodulating  
567 *Bradyrhizobium* strains, among which is the DOA9 strain (Noisangiam *et al.*, 2012;  
568 Teamtisong *et al.*, 2014). As *A. americana* belongs to the most basal lineage in the  
569 *Aeschynomene* phylogeny, it may be representative of the ancestral symbiotic mechanisms  
570 found in the genus. On the other hand, *A. patula* has a restricted Madagascan distribution with  
571 only one accession being available, but it is of interest due to its relatively smaller plant size  
572 and genome size (actually the smallest diploid genome in the group) making this species the  
573 “Arabidopsis” of the genus *Aeschynomene*. As for *A. americana*, this species is efficiently  
574 nodulated by non-photosynthetic bradyrhizobia, but it is also compatible with the  
575 photosynthetic *nod* gene-containing ORS285 strain. This property makes *A. patula*

576 particularly interesting as it allows direct comparisons of mechanisms and pathways between  
577 it and *A. evenia* without the problem of potential strain effects on symbiotic responses. In  
578 addition, when considering the *Aeschynomene* phylogeny, *A. patula* is more closely related to  
579 *A. evenia* than is *A. americana*, and so it may be more suitable to demonstrate the changes  
580 necessary to switch a Nod-dependent to a Nod-independent process or vice-versa. Developing  
581 sequence resources and functional tools for *A. americana* and/or *A. patula* is now necessary to  
582 set up a fully workable comparative *Aeschynomene* system. In the long run, handling such a  
583 genetic system will be instrumental in understanding how photosynthetic *Bradyrhizobium* and  
584 some *Aeschynomene* species co-evolved and in unravelling the molecular mechanisms of the  
585 Nod-independent symbiosis.

586

587

## 588 **ACKNOWLEDGMENTS**

589 We thank the different seed banks and herbaria for provision of seeds and herbarium vouchers  
590 that were used in this study. The present work has benefited from the facilities and expertise  
591 of the cytometry facilities of Imagerie-Gif ([http://www.i2bc.paris-](http://www.i2bc.paris-saclay.fr/spip.php?article279)  
592 [saclay.fr/spip.php?article279](http://www.i2bc.paris-saclay.fr/spip.php?article279)) and of the molecular cytogenetic facilities of the AGAP  
593 laboratory (<http://umr-agap.cirad.fr/en/plateformes/plateau-de-cytogenetique-moleculaire>).  
594 This work was supported by a grant from the French National Research Agency (ANR-  
595 AeschyNod-14-CE19-0005-01) that financed the design of the study, experimentation and  
596 analysis of the data.

597

598

## 599 **AUTHOR CONTRIBUTIONS**

600 J.F.A. designed the experiments. L.B., C.C., R.R., J.F., M.G.M, S.C.B., C.H., M.D. and J.F.A.  
601 performed the experiments and obtained the data. P.S., C.S., L.M. undertook the phylogenetic  
602 analyses. P.M., J.Q., G.P.L., X.P., A.D'H., E.G. and J.F.A. analysed the data. M.G., R.D., H.  
603 Randriambanona, H. Ramanankierna, H.V. and M.Z. contributed to the acquisition and  
604 analysis of accessions. J.F.A. wrote the paper. L.B. and C.C contributed equally. All authors  
605 read and approved the final manuscript.

606

607

## 608 **REFERENCES**

609

- 610 **Alazard D. 1985.** Stem and root nodulation in *Aeschynomene* spp. *Applied and*  
611 *Environmental Microbiology* **50**: 732-734.
- 612 **Alazard D, Duhoux E. 1987.** Nitrogen-fixing stem nodules on *Aeschynomene afraspera*.  
613 *Biological fertility Soils*. **4**: 61-66.
- 614 **Arrighi JF, Cartieaux F, Brown SC, Rodier-Goud M, Boursot M, Fardoux J, Patrel D,**  
615 **Gully D, Fabre S, Chaintreuil C et al. 2012.** *Aeschynomene evenia*, a Model Plant for  
616 Studying the Molecular Genetics of the Nod-Independent Rhizobium-Legume Symbiosis.  
617 *Molecular Plant-Microbe Interactions* **25**: 851-861.
- 618 **Arrighi JF, Cartieaux F, Chaintreuil C, Brown SC, Boursot M, Giraud E. 2013.**  
619 Genotype delimitation in the Nod-independent model legume *Aeschynomene evenia*. *PloS*  
620 *One* **8**:e63836.
- 621 **Arrighi JF, Chaintreuil C, Cartieaux F, Cardi C, Rodier-Goud M, Brown SC, Boursot**  
622 **M, d’Hont A, Dreyfus B, Giraud E. 2014.** Radiation of the Nod-independent *Aeschynomene*  
623 relies on multiple allopolyploid speciation events. *New Phytologist* **201**: 1457-68.
- 624 **Arrighi JF, Cartieaux F. 2015.** Out of water of a new model legume: the Nod-independent  
625 *Aeschynomene evenia*. In *Biological Nitrogen Fixation*, Vol 2 Ed. de Bruijn. Wiley-Blackwell  
626 publishers. Chapter **45**, 447-54.
- 627 **Behm JE, Geurts R, Kiers ET. 2014.** *Parasponia*: a novel system for studying mutualism  
628 stability. *Trends Plant Sci* **19**: 757-63.
- 629 **Boivin C, Ndoye I, Molouba F, De Lajudie P, Dupuy N, Dreyfus B. 1997.** Stem nodulation  
630 in legumes: diversity, mechanisms, and unusual characteristics. *Critical Reviews in Plant*  
631 *Sciences* **16**: 1-30.
- 632 **Bonaldi K, Gargani D, Prin Y, Fardoux J, Gully D, Nouwen N, Goormachtig S, Giraud**  
633 **E. 2011.** Nodulation of *Aeschynomene afraspera* and *A. indica* by photosynthetic  
634 *Bradyrhizobium* sp. strain ORS285: The Nod-dependent versus the Nod-independent  
635 symbiotic interaction. *M.P.M.I.* **24**: 1359-1371.
- 636 **Bravo A, York T, Pumplun N, Mueller LA, Harrison MJ. 2016.** Genes conserved for  
637 arbuscular mycorrhizal symbiosis identified through phylogenomics. *Nat Plants* **18**: 15208.
- 638 **Chaintreuil C, Arrighi JF, Giraud E, Miché L, Moulin L, Dreyfus B, Munive-Hernandez**  
639 **J, Villegas-Hernandez M, Béna G. 2013.** Evolution of symbiosis in the legume genus  
640 *Aeschynomene*. *New Phytologist* **200**:1247-59.
- 641 **Chaintreuil C, Rivallan R, Bertoli DJ, Klopp C, Gouzy J, Courtois B, Leleux P, Martin**  
642 **G, Rami JF, Gully D et al. 2016a.** A gene-based map of the Nod factor-independent

- 643 *Aeschynomene evenia* sheds new light on the evolution of nodulation and legume genomes.  
644 *DNA Res* **23**:365-76.
- 645 **Chaintreuil C, Gully J, Hervouet C, Tittabutr P, Randriambanona H, Brown SC, Lewis**  
646 **GP, Bourge M, Cartieaux F, Boursot M et al. 2016b.** The evolutionary dynamics of  
647 ancient and recent polyploidy in the African semi-aquatic species of the legume genus  
648 *Aeschynomene*. *New Phytologist* **211**:1077-91.
- 649 **Chaintreuil C, Perrier X, Martin G, Fardoux J, Lewis GP, Brottier L, Rivallan R,**  
650 **Gomez-Pacheco M, Bourges M, Lamy L et al. 2018.** Naturally occurring variations in the  
651 nod-independent model legume *Aeschynomene evenia* and relatives: a resource for  
652 nodulation genetics. *BMC Plant Biol.* **18**:54.
- 653 **Czernic P, Gully D, Cartieaux F, Moulin L, Guefrachi I, Patrel D, Pierre O, Fardoux J,**  
654 **Chaintreuil C, Nguyen P et al. 2015.** Convergent Evolution of Endosymbiont Differentiation  
655 in Dalbergioid and Inverted Repeat-Lacking Clade Legumes Mediated by Nodule-Specific  
656 Cysteine-Rich Peptides. *Plant Physiol* **169**: 1254-65.
- 657 **Cook, B.G., Pengelly, B.C., Brown, S.D., Donnelly, J.L., Eagles, D.A., Franco, M.A.,**  
658 **Hanson, J., Mullen, B.F., Partridge, I.J., Peters, M. and Schultze-Kraft, R. 2005.** Tropical  
659 Forages: an interactive selection tool. CSIRO, DPI&F(Qld), CIAT and ILRI, Brisbane,  
660 Australia. <http://www.tropicalforages.info>
- 661 **Dereeper A, Homa F, Andres G, Sempere G, Sarah G, Hueber Y, Dufayard JF, Ruiz M.**  
662 **2015.** SNIPlay3: a web-based application for exploration and large scale analyses of genomic  
663 variations. *Nucleic Acids Res* **43**(W1):W295-300.
- 664 **Delaux PM, Varala K, Edger PP, Coruzzi GM, Pires JC, Ané JM. 2014.** Comparative  
665 phylogenomics uncovers the impact of symbiotic associations on host genome evolution.  
666 *PLoS Genet* **10**: e1004487.
- 667 **Delaux PM, Radhakrishnan G, Oldroyd G. 2015.** Tracing the evolutionary path to  
668 nitrogen-fixing crops. *Curr Opin Plant Biol* **26**: 95-9.
- 669 **Du Puy DJ, Labat J-N, Rabevohitra R, Villiers J-F, Bosser J, Moat J. 2002.** The  
670 *Leguminosae* of Madagascar. *Royal Botanic Gardens, Kew.*
- 671 **Fabre S, Gully D, Poitout A, Patrel D, Arrighi JF, Giraud E, Czernic P, Cartieaux F.**  
672 **2015.** Nod Factor-Independent Nodulation in *Aeschynomene evenia* Required the Common  
673 Plant-Microbe Symbiotic Toolkit. *Plant Physiol* **169**: 2654-64.
- 674 **Geurts R, Xiao TT, Reinhold-Hurek B. 2016.** What Does It Take to Evolve A Nitrogen-  
675 Fixing Endosymbiosis? *Trends Plant Sci* **21**:199-208.

- 676 **Gillett JB, Polhill RM, Verdcourt B. 1971.** Leguminosae (part 3): subfamily Papilionoideae  
677 (part 1). In Milne-Redhead E & Polhill RM (eds). Flora of Tropical East Africa. *Royal*  
678 *Botanic Gardens, Kew.*
- 679 **Giraud E, Hannibal L, Fardoux J, Vermeglio A, Dreyfus B. 2000.** Effect of  
680 *Bradyrhizobium* photosynthesis on stem nodulation of *Aeschynomene sensitiva*. *P.N.A.S.* **97**:  
681 14795-14800.
- 682 **Giraud E, Moulin L, Vallenet D, Barbe V, Cytryn E, Avarre JC, Jaubert M, Simon D,**  
683 **Cartieaux F, Prin Y, et al. 2007.** Legumes symbioses: absence of Nod genes in  
684 photosynthetic bradyrhizobia. *Science* **316**: 1307-1312.
- 685 **Garsmeur O, Droc G, Antonise R, Grimwood J, Potier B, Aitken K, Jenkins J, Martin**  
686 **G, Charron C, Hervouet C et al. 2018.** A mosaic monoploid reference sequence for the  
687 highly complex genome of sugarcane. *Nature Communications* **9**:2638.
- 688 **Govindarajulu R, Hughes CE, Alexander PJ, Bailey CD. 2011.** The complex evolutionary  
689 dynamics of ancient and recent polyploidy in *Leucaena* (Leguminosae; Mimosoideae). *Am J*  
690 *Bot* **98**:2064-76.
- 691 **Griesmann M, Chang Y, Liu X, Song Y, Haberer G, Crook MB, Billault-Penneteau B,**  
692 **Lauressergues D, Keller J, Imanishi L et al. 2018.** Phylogenomics reveals multiple losses  
693 of nitrogen-fixing root nodule symbiosis. *Science* **361**(6398). pii: eaat1743.
- 694 **Hagerup O. 1928.** En hygrofil baelplante (*Aeschynomene aspera* L.) med bakterieknolde  
695 paa staenglen. *Dansk Bot. Arkiv.* **14**: 1-9.
- 696 **Howieson J.G. and Dilworth M.J. (Eds.). 2016.** Working with rhizobia. Australian Centre  
697 for International Agricultural Research: Canberra.
- 698 **Katoh K, Standley DM. 2013.** MAFFT multiple sequence alignment software version 7:  
699 improvements in performance and usability. *Mol Biol Evol* **30**:772-80.
- 700 **Klitgaard, B.B. & Lavin, M. 2005.** Tribe Dalbergieae *sens. lat.* In G. Lewis *et al.* (eds.)  
701 Legumes of the World. *Royal Botanic Gardens, Kew.* 307-335.
- 702 **Lartillot N, Philippe H. 2004.** A Bayesian Mixture Model for Across-Site Heterogeneities in  
703 the Amino-Acid Replacement Process. *Mol Biol Evol* **21**:1095-1109.
- 704 **Lavin M, Pennington RT, Klitgaard BB, Spretnt JI, de Lima HC, Gasson PE. 2001.** The  
705 dalbergioid legumes (Fabaceae): delimitation of a pantropical monophyletic clade. *Am J Bot*  
706 **88**: 503-533.
- 707 **Lewis G, Schrire B, Mackinder B, Lock M. 2005.** Legumes of the world. *Royal Botanic*  
708 *Gardens, Kew.*
- 709 **Lock JM. 1989.** Legumes of Africa. A check-list. *Royal Botanic Gardens, Kew, England.*

- 710 **Loureiro MF, De Faria SM, James EK, Pott A, Franco AA. 1994.** Nitrogen-Fixing Stem  
711 Nodules of the Legume, *Discolobium Pulchellum* Benth. *New Phytologist* **128**: 283-295.
- 712 **Loureiro MF, James EK, Sprent JI, Franco AA. 1995.** Stem and root nodules on the  
713 tropical wetland legume *Aeschynomene fluminensis*. *New Phytologist* **130**: 531-544.
- 714 **LPWG (The Legume Phylogeny Working Group). 2017.** A new subfamily classification of  
715 the Leguminosae based on a taxonomically comprehensive phylogeny. *Taxon* **66**: 44-77.
- 716 **Madsen LH, Tirichine L, Jurkiewicz A, Sullivan JT, Heckmann AB, Bek AS, Ronson  
717 CW, James EK, Stougaard J. 2010.** The molecular network governing nodule  
718 organogenesis and infection in the model legume *Lotus japonicus*. *Nature Communication* **1**:  
719 10.
- 720 **Miché L, Moulin L, Chaintreuil C, Contreras-Jimenez JL, Munive-Hernandez JA, Del  
721 Carmen Villegas-Hernandez M, Crozier F, Béna G. 2010.** Diversity analyses of  
722 *Aeschynomene* symbionts in Tropical Africa and Central America reveal that nod-independent  
723 stem nodulation is not restricted to photosynthetic bradyrhizobia. *Environ Microbiol* **12**:  
724 2152-2164.
- 725 **Molouba, F, Lorquin J, Willems A, Hoste B, Giraud E, Dreyfus B, Gillis M, DeLajudie P  
726 and Masson-Boivin C. 1999.** "Photosynthetic bradyrhizobia from *Aeschynomene* spp. are  
727 specific to stem-nodulated species and form a separate 16S ribosomal DNA restriction  
728 fragment length polymorphism group." *Applied and Environmental Microbiology* **65**: 3084-  
729 3094.
- 730 **Noisangiam R, Teamtisong K, Tittabutr P, Boonkerd N, Toshiki U, Minamisawa K,  
731 Teaumroong N. 2012.** Genetic diversity, symbiotic evolution, and proposed infection process  
732 of *Bradyrhizobium* strains isolated from root nodules of *Aeschynomene americana* L. in  
733 Thailand. *Appl Environ Microbiol* **78**:6236-50.
- 734 **Nouwen N, Arrighi JF, Cartieaux F, Gully D, Klopp C, Giraud E. 2017.** The role of  
735 rhizobial (NifV) and plant (FEN1) homocitrate synthesis in *Aeschynomene* - photosynthetic  
736 *Bradyrhizobium* symbiosis. *Scientific Reports*, **7**: 448.
- 737 **Okazaki S, Kaneko T, Sato S, Saeki K. 2013.** Hijacking of leguminous nodulation signaling  
738 by the rhizobial type III secretion system. *P.N.A.S.* **110**:17131-6.
- 739 **Okazaki S, Tittabutr P, Teulet A, Thouin J, Fardoux J, Chaintreuil C, Gully D, Arrighi  
740 JF, Furuta N, Miwa H et al. 2015.** Rhizobium-legume symbiosis in the absence of Nod  
741 factors: two possible scenarios with or without the T3SS. *ISME J* **10**: 64-74.



- 742 **Okubo T, Fukushima S, Minamisawa K. 2012.** Evolution of *Bradyrhizobium-*  
743 *Aeschynomene* mutualism: living testimony of the ancient world or highly evolved state?  
744 *Plant & Cell Physiology* **53**:2000-2007.
- 745 **Okuyama Y, Tanabe AS, Kato M. 2012.** Distinguishing ancient allotetraploidization in Asian  
746 *Mitella*: an integrated approach for multilocus combinations. *Mol Biol Evol* **29**: 429-39.
- 747 **Revell LJ. 2012.** Phytools: An R package for phylogenetic comparative biology (and other  
748 things). *Methods Ecol. Evol* **3**: 217-223.
- 749 **Oueslati A, Salhi-Hannachi A, Luro F, Vignes H, Mournet P, Ollitrault P. 2017.**  
750 Genotyping by sequencing reveals the interspecific *C. maxima* / *C. reticulata* admixture along  
751 the genomes of modern citrus varieties of mandarins, tangors, tangelos, orangelos and  
752 grapefruits. *PLoS One* **12**:e0185618.
- 753 **Rudd VE. 1955.** The American species of *Aeschynomene*. *Contributions of the United States*  
754 *National Herbarium* **32**: 1-172.
- 755 **Rudd VE 1981.** *Aeschynomeneae*. In: Polhill RM, Raven PH eds. *Advances in legume*  
756 *systematics*. Kew: Royal Botanic Gardens. **Part1**: 347-354.
- 757 **Sprent JI, James EK. 2008.** Legume-rhizobial symbiosis: an anorexic model? *New*  
758 *Phytologist* **179**: 3-5.
- 759 **Sprent JI, Ardley J, James EK. 2017.** Biogeography of nodulated legumes and their  
760 nitrogen-fixing symbionts. *New Phytologist* doi: 10.1111/nph.14474.
- 761 **Teamtisong K, Songwattana P, Noisangiam R, Piromyou P, Boonkerd N, Tittabutr P,**  
762 **Minamisawa K, Nantagij A, Okazaki S, Abe M, Uchiumi T, Teaumroong N. 2014.**  
763 Divergent nod-containing *Bradyrhizobium* sp. DOA9 with a megaplasmid and its host range.  
764 *Microbes Environ.* **29**: 370-6.
- 765 **To TH, Scornavacca C. 2015.** Efficient algorithms for reconciling gene trees and species  
766 networks via duplication and loss events. *BMC Genomics* **16** Suppl 10:S6.
- 767 **van Velzen R, Holmer R, Bu F, Rutten L, van Zeijl A, Liu W, Santuari L, Cao Q,**  
768 **Sharma T, Shen D et al. 2018.** Comparative genomics of the nonlegume *Parasponia* reveals  
769 insights into evolution of nitrogen-fixing rhizobium symbioses. *PNAS* **115**:E4700-E4709.
- 770 **Whitfield JB, Lockhart PJ. 2007.** Deciphering ancient rapid radiations. *Trends in Ecology*  
771 *and Evolution* **22**: 258-265.

772

773

774 **FIGURE LEGENDS**

775

776 **Figure 1: Phylogeny of the genus *Aeschynomene* and allied genera.**

777 The Bayesian phylogenetic reconstruction was obtained using the concatenated *ITS* (Internal  
778 Transcribed Spacer) + *matK* sequences. Numbers at branches indicate posterior probability  
779 above 0.5. The five main lineages are identified with a circled number and the two previously  
780 studied *Aeschynomene* groups are framed in a red box bordered with a dashed line. On the  
781 right are listed *Aeschynomene* subgenus *Aeschynomene* (in green), other *Aeschynomene*  
782 subgenera or species groups (in blue) and related genera (in orange).

783

784 **Figure 2: Genomic characteristics and phylogenetic relationships.**

785 (a) Simplified Bayesian *ITS+matK* phylogeny with representative species of different lineages  
786 and groups. The *A. evenia*, *A. afraspera* and BRH (*Bakerophyton-Rueppelia-Humularia*)  
787 clades are represented by black triangles and the polytomy is depicted in bold. Chromosome  
788 numbers are indicated in brackets. (b) Phylogenetic relationships based on the combination of  
789 4 concatenated nuclear low-copy genes (*CYP1*, *eif1a*, *SuSy* and *TIP1;1* genes detailed in  
790 Figure S5). Diploid species ( $2n=20$ ) are in blue, polyploid species ( $2n\geq 28$ ) in black. The A  
791 and B subgenomes of the polyploid taxa are delineated by red and green boxes in dashed  
792 lines, respectively. Nodes with a posterior probability inferior to 0.5 were collapsed into  
793 polytomies. Posterior probability above 0.5 are indicated at every node. (c) The one-  
794 allopolyploidisation hypothesis (N1-best) obtained with the phylogenetic network analysis  
795 based on the T2 tree with reticulations in blue (detailed in Fig. S7).

796

797 **Figure 3: Occurrence of adventitious root primordia and of stem nodulation.**

798 (a) Simplified Bayesian *ITS+matK* phylogeny of the whole group with the *A. evenia*, *A.*  
799 *afraspera* and BRH (*Bakerophyton-Rueppelia-Humularia*) clades represented by black  
800 triangles. The polytomy is depicted in bold. The shared presence of adventitious root  
801 primordia is depicted on the stem by a blue circle. Dashed red boxes indicate groups  
802 comprising aerial stem-nodulating species. Asterisks refer to illustrated species in (b) for  
803 aerial stem-nodulation. (b) Stems of representatives for the different lineages and groups.  
804 Small spots on the stem correspond to dormant adventitious root primordia and stem nodules  
805 are visible on the species marked by an asterisk. Bars: 1cm.

806

807 **Figure 4: Comparison of the root nodulation properties.**

808 (a) Species of different lineages and groups that were tested for nodulation are listed in the  
809 simplified Bayesian phylogeny on the left. Root nodulation tests were performed using the



810 DOA9, ORS285, ORS285 $\Delta$ *nod* and ORS278 strains. E, effective nodulation; e, partially  
811 effective nodulation; i, ineffective nodulation, -, no nodulation; blank, not tested. (b) Number  
812 of nodules per plant, (c) relative acetylene-reducing activity (ARA) and (d) aspect of the  
813 inoculated roots developing nodules or not (some nodules were cut to observe the  
814 leghemoglobin color inside) after inoculation with *Bradyrhizobium* DOA9, ORS285 and  
815 ORS278 on *A. americana*, *A. patula*, *A. afraspera* and *A. evenia*. Error bars in (b) and (c)  
816 represent s.d. (n=6). Scale bar in (d): 1 mm.

817

818 **Figure 5: Characteristics of diploid species.**

819 (a) Development and germplasm data for species that are listed in the simplified phylogeny on  
820 the left. *A. evenia* from the Nod-independent clade (NI) is also included for comparison.  
821 Germplasm numbers correspond to the sum of accessions available at CIAT, USDA, Royal  
822 Botanic Gardens (Kew), AusPGRIS, IRRI and at LSTM. (b) Multi-dimensional scaling  
823 (MSD) plots of the genetic diversity among *A. americana* (left) and *A. villosa* (right)  
824 accessions according to coordinates 1 and 2 (C1, C2). Identified groups are delimited by  
825 circles and labeled with numbers. (c) Geographical distribution of the of *A. americana* and  
826 *A. villosa* accessions. Taxon colours and group numbers are the same as in (b). Details of the  
827 accessions are provided in Table S4.

828

829 **Figure S1: *matK* phylogeny of the genus *Aeschynomene* and allied genera.**

830 Bayesian phylogenetic reconstruction obtained using the chloroplast *matK* gene. Numbers at  
831 branches are posterior probability.

832

833 **Figure S2: *ITS* phylogeny of the genus *Aeschynomene* and allied genera.**

834 Bayesian phylogenetic reconstruction obtained using the Internal Transcribed Spacer (*ITS*)  
835 sequence. Numbers at branches are posterior probability.

836

837 **Figure S3: Chromosome numbers in *Aeschynomene* species.**

838 Root tip metaphase chromosomes stained in blue with DAPI (4',6-diamidino-2-phenylindole).  
839 Chromosome numbers are indicated in brackets. Scale bars: 5  $\mu$ m.

840

841 **Figure S4: Chromosome numbers in species of genera related to *Aeschynomene***

842 Root tip metaphase chromosomes stained in blue with DAPI (4',6-diamidino-2-phenylindole).  
843 Chromosome counts are indicated in brackets. Scale bars: 5  $\mu$ m.

844

845 **Figure S5: Phylogenetic trees based on nuclear low-copy genes.**

846 Bayesian phylogenetic reconstructions obtained for the *CYP1*, *eif1a*, *SuSy* and *TIP1;1* genes.  
847 Diploid species ( $2n=20$ ) are in blue, polyploid species ( $2n\geq 28$ ) in black excepted *A. afraspera*  
848 for which the A and B gene copies are distinguished in red and green respectively. -A, -A1, -  
849 A2, -B, -B1 and -B2 indicated the different copies found. Putative A and B subgenomes of the  
850 polyploid taxa are delineated by red and green boxes in dashed lines, respectively. Numbers at  
851 branches represent posterior probability.

852

853 **Figure S6: Ancestral state reconstruction of ploidy levels in the genus *Aeschynomene***  
854 **and allied genera.**

855 Ancestral state reconstruction was estimated in SIMMAP software using the 50% majority-  
856 rule topology obtained by Bayesian analysis of the combined *ITS+matK* sequences. Ploidy  
857 levels are indicated by different colors. Unknown ploidy levels are denoted by a dash.

858

859 **Figure S7: Phylogenetic networks based on the four nuclear *CYP1*, *eif1a*, *SuSy* and**  
860 ***TIP1;1* genes.**

861 (a) No-allopolyploidisation hypothesis (T1) based on the concatenated gene tree obtained  
862 taking into account the group A (Fig. 2b). (b) No-allopolyploidisation hypothesis (T2) based  
863 on the concatenated gene tree obtained taking into account the group B (Fig. 2b). (c) One-  
864 allopolyploidisation hypothesis (N1-best). (d) Two-allopolyploidisation hypothesis (N2-best).  
865 Blue lines indicate reticulations while other nodes of the network are associated to speciation  
866 events. Reconciliation scores obtained for each phylogenetic network are indicated.

867

868 **Figure S8: Ancestral state reconstruction of adventive root primordia in the genus**  
869 ***Aeschynomene* and allied genera.**

870 Ancestral state reconstruction was estimated in SIMMAP software using the 50% majority-  
871 rule topology obtained by Bayesian analysis of the combined *ITS+matK* sequences. Data on  
872 the adventitious root primordia come from the present analysis and pertinent previously  
873 published data. Presence or not of adventitious root primordia is indicated by different colors.

874

875 **Figure S9: Ancestral state reconstruction of ecological habit in the genus *Aeschynomene***  
876 **and allied genera.**

877 Ancestral state reconstruction was estimated in SIMMAP software using the 50% majority-  
878 rule topology obtained by Bayesian analysis of the combined *ITS+matK* sequences. Data on  
879 the species ecology come from pertinent previously published data. Ecological habits are  
880 indicated by different colors.

881

882 **Figure S10: Ancestral state reconstruction of the aerial stem nodulation ability in the**  
883 **genus *Aeschynomene* and allied genera.**

884 Ancestral state reconstruction was estimated in SIMMAP software using the 50% majority-  
885 rule topology obtained by Bayesian analysis of the combined *ITS+matK* sequences. Data on  
886 the occurrence of stem nodulation come from pertinent previously published data. Occurrence  
887 or not of stem nodulation is indicated by different colors.

888

889 **Figure S11: Ancestral state reconstruction of the ability to nodulate with the**  
890 **photosynthetic *Bradyrhizobium* strains in the genus *Aeschynomene* and allied genera.**

891 Ancestral state reconstruction was estimated in SIMMAP software using the 50% majority-  
892 rule topology obtained by Bayesian analysis of the combined *ITS+matK* sequences. Data on  
893 nodulation with photosynthetic *Bradyrhizobium* strains come from the present analysis and  
894 pertinent previously published data. Nodulation with photosynthetic *Bradyrhizobium* strains is  
895 considered positive only if reported as occurring naturally or being efficient *in vitro*.

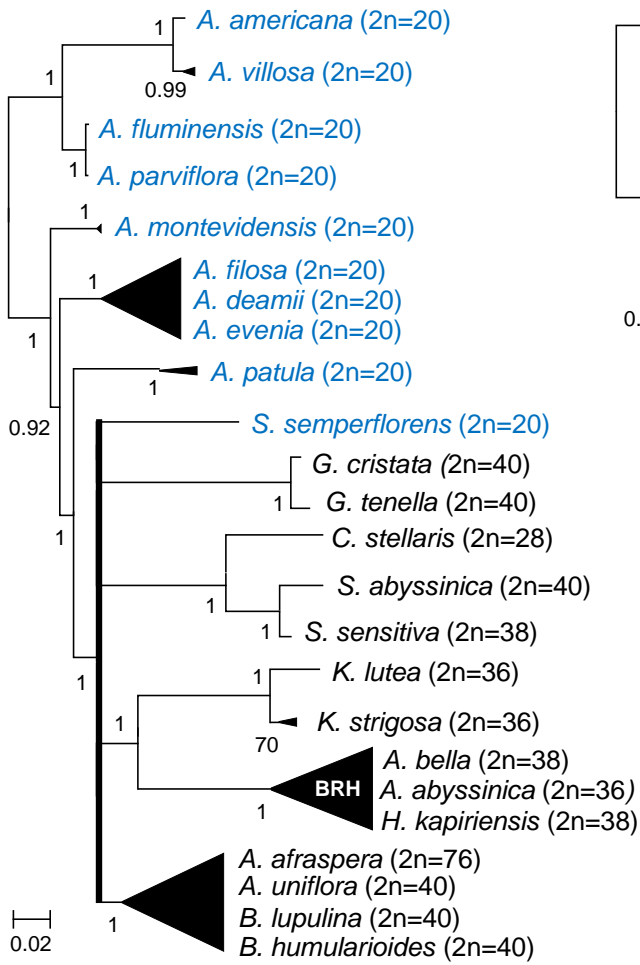
896

897 **Figure S12: Ancestral state reconstruction of the ability to nodulate with the**  
898 **photosynthetic *Bradyrhizobium* strain ORS278 in the genus *Aeschynomene* and allied**  
899 **genera.**

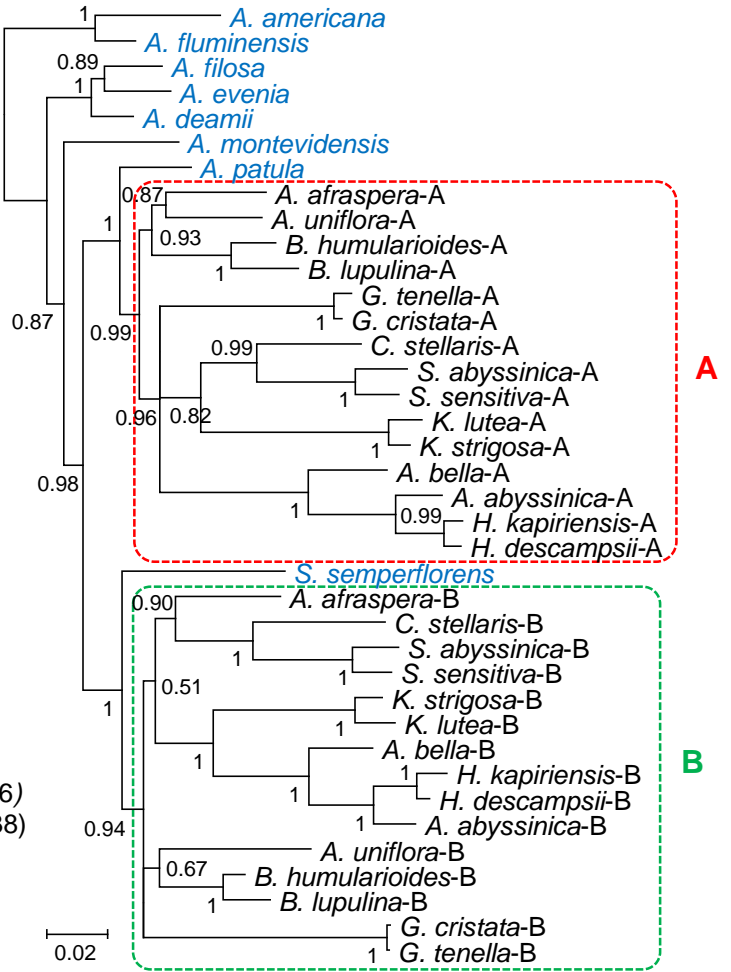
900 Ancestral state reconstruction was estimated in SIMMAP software using the 50% majority-  
901 rule topology obtained by Bayesian analysis of the combined *ITS+matK* sequences. Data on  
902 nodulation with ORS278 come from the present analysis and pertinent previously published  
903 data. Ability or not to nodulate with ORS278 is indicated by different colors.



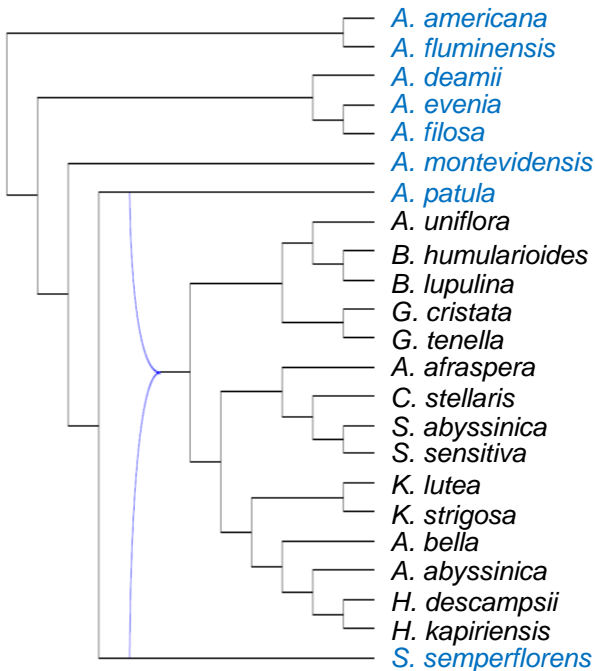
**a ITS + matK**

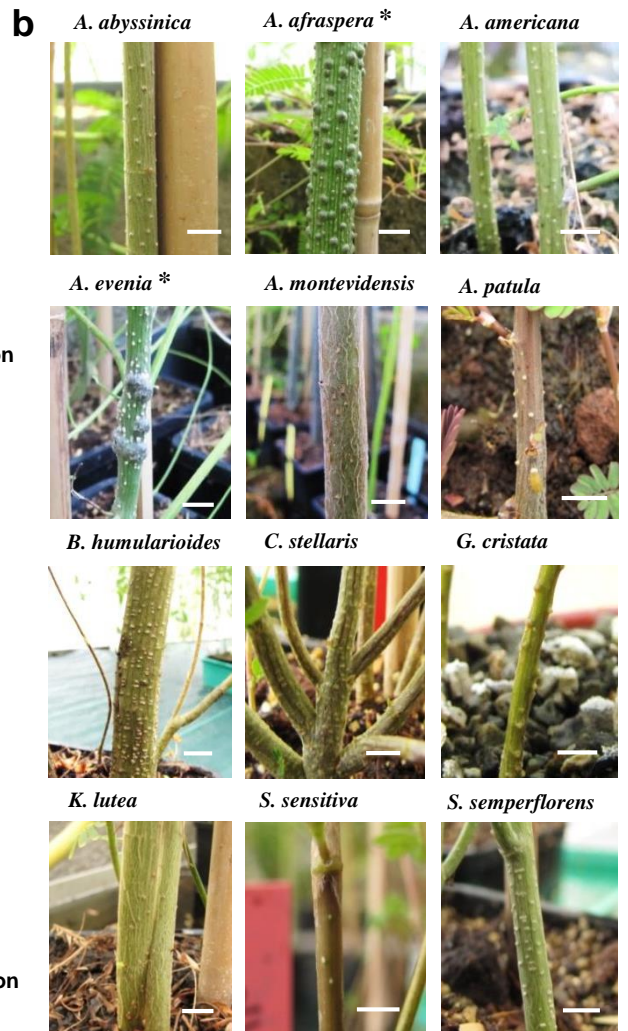
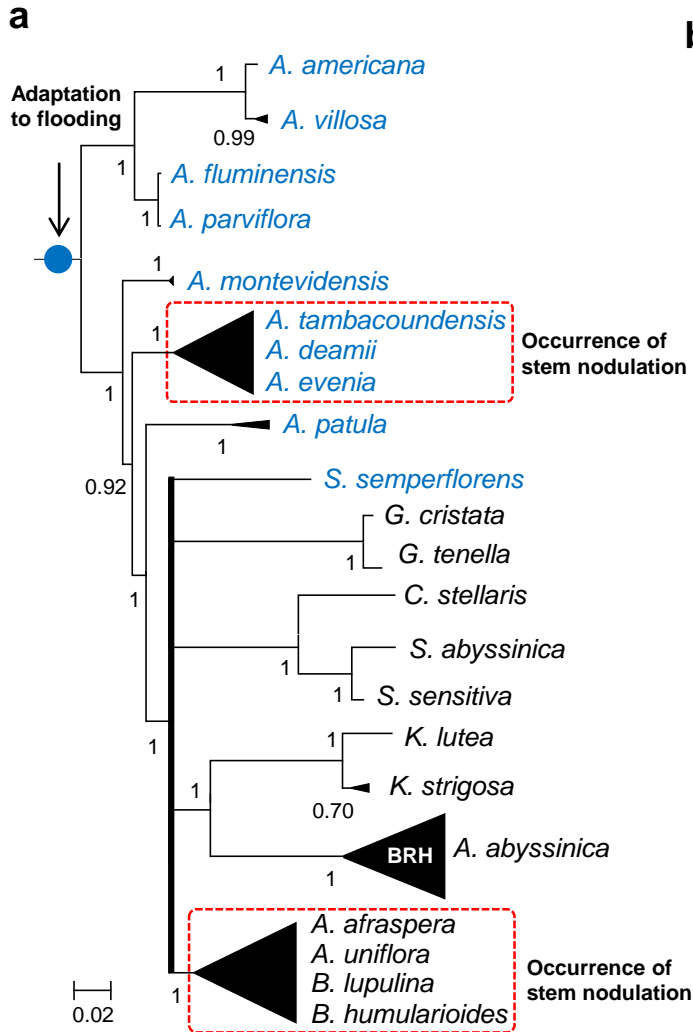


**b Concatenated nuclear genes**

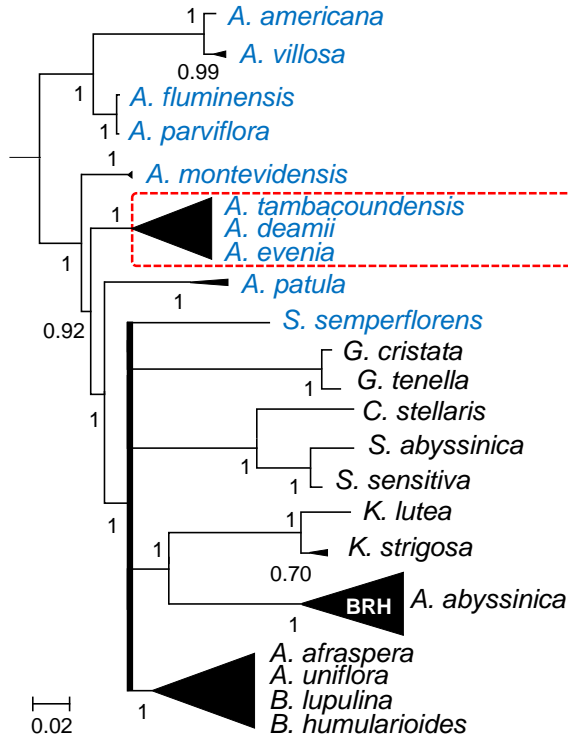


**C Phylogenetic network**

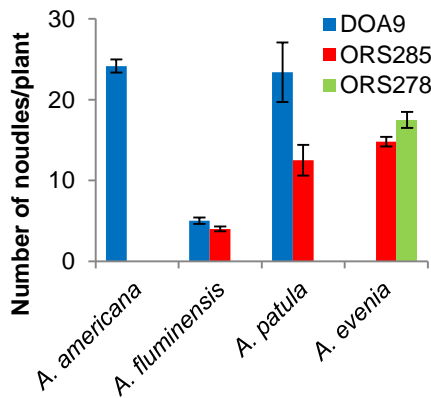
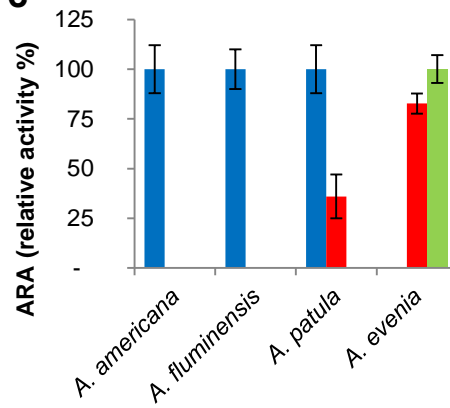






**a**

Species	DOA9	ORS285	ORS285 $\Delta nod$	ORS278
<i>A. americana</i>	E	-	-	-
<i>A. villosa</i>	E	-	-	-
<i>A. fluminensis</i>	E	i	-	-
<i>A. parviflora</i>	E	-	-	-
<i>A. montevidensis</i>	-	-	-	-
<i>A. tambacoundensis</i>	-	E	E	E
<i>A. deamii</i>	-	E	E	E
<i>A. evenia</i>	-	E	E	E
<i>A. patula</i>	E	e	-	-
<i>S. semperflorens</i>	-	-	-	-
<i>G. cristata</i>	E	-	-	-
<i>G. tenella</i>	E	-	-	-
<i>C. stellaris</i>	E	i	-	-
<i>S. abyssinica</i>	E	i	-	-
<i>S. sensitiva</i>	-	-	-	-
<i>K. lutea</i>	i	-	-	-
<i>K. strigosa</i>	i	-	-	-
<i>A. abyssinica</i> (BRH)	i	-	-	-
<i>A. afraspera</i>	E	E	-	-
<i>A. uniflora</i>	i	i	-	-
<i>B. lupulina</i>	i	-	-	-
<i>B. humularioides</i>	i	-	-	-

**b****c****d**